ELSEVIER

Contents lists available at ScienceDirect

# Spectrochimica Acta Part B: Atomic Spectroscopy

journal homepage: www.elsevier.com/locate/sab

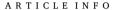


Invited Review

# Laser-ablation absorption spectroscopy: Reviewing an uncommon hyphenation

Jonathan Merten

Department of Chemistry and Physics, Arkansas State University, Jonesboro, AR, United States



Keywords: LA-AAS Plasma diagnostics Isotope ratio Absolute quantitation Absorption spectroscopy High-resolution spectroscopy



Absorption spectroscopy hyphenations of the laser-induced plasma have been attempted by a handful of groups since the early 1990s. Despite the measurement's relatively long history, there are few reviews and the details of the experiment remain somewhat opaque. Though the early experiments were directed at understanding laser-induced deposition physics, more recent measurements have begun to bend absorption spectroscopy to plasma diagnostics with an eye to analytical chemistry applications of laser ablation. This review discusses the benefits and difficulties of the different experimental approaches in addition to analytical and plasma characterization applications. Because the laser-induced plasma is so different from the usual atomic reservoirs used for atomic absorption spectroscopy, the assumptions of the Beer-Lambert Law are also discussed. Finally, with several groups currently working in the field, I provide an outlook for the future of the measurements.

# 1. Introduction

The laser-induced plasma (LIP) is important to chemical analysis, material science, electronics, physical chemistry, astronomy, plasma science and fundamental physics studies. The plasmas themselves are complex and fleeting, a combination that has both tantalized and frustrated generations of researchers. Optically, the push to understand their formation and evolution began with passive observation of thermal emission spectra. However, these measurements probe only excited states and do not provide direct information about the ground or metastable states.

Extrapolating from emission measurements to understand the full atomic state distribution function (ASDF) is fraught. Nonetheless, assumption of some form of thermal equilibrium is often used to extrapolate from emission measurements to a full characterization of the plasma. However, as many authors point out (e.g. References [1, 2]), even with the simplifying assumption of local thermodynamic equilibrium (LTE), plasma characterization via emission is still complicated by spatial inhomogeneity in the equilibrium temperature. Additionally, LTE only allows *relative* quantitation of species via thermal emission data- absolute measurements require complex calibration of the absolute spectral irradiance response of the entire optical system. Finally, LTE is clearly absent in important cases- e.g. times greater than a few microseconds or in reduced-pressure environments. Absent LTE,

complex collisional-radiative models result in an even more difficult interpretation.

More recently, tunable lasers have allowed fluorescence and absorption spectroscopy measurements of the LIP. Unlike thermal techniques, absorption spectroscopy can directly probe ground or excited (including metastable) states. Where fluorescence and thermal emission spectroscopy require calibration of the absolute spectral radiance response of the optical system to quantitate a given state directly (i.e. number density or mass), absorption spectroscopy does not, albeit with introduction of a separate set of experimental complexities. Additionally, the absorbance measurement geometry is a well-defined line-ofsight when the probe source is coherent, simplifying data interpretation. Finally, where the informing power of LIP emission is limited by the high density of overlapping and broadened peaks at thermally emissive times, absorption spectroscopy can probe the LIP when peaks are narrow and the atomic state distribution function (and resulting absorption spectrum) is simplified. Of course, the richness of information in the thermal emission plasma is also lost.

Continuum-source absorption spectroscopy has been widely used in the physics community to study plasmas at UV and XUV wavelengths, and has been reviewed by Costello et al. in this context [3]. Within the analytical spectroscopy community, Omenetto and Hahn mention absorption spectroscopy in their review of plasma diagnostics and Gornushkin and Panne's contemporaneous review of pump-probe plasma

E-mail address: jmerten@astate.edu.

 $<sup>^{\</sup>ast}$  Corresponding author,

diagnostics also includes a brief section on absorption spectroscopy [4,5]. Harilal et al. treat laser-ablation absorption spectropy (LA-AS) alongside LA-laser-induced fluorescence (LA-LIF) and laser-induced breakdown spectroscopy (LIBS) in the context of isotope ratio measurements in a more recent review centered around isotopic measurements in the LIP [6]. The present review is dedicated to the principles, methods and findings of laser-ablation absorption spectroscopy or laserablation atomic absorption spectroscopy (LA-AAS), with special emphasis on its use as a quantitative tool or for diagnostics aimed at improving the LIP as a quantitative tool. There is now more than a quarter century of work in LA-AS, with many developments in the past decade. Although the related laser-ablation laser-induced fluorescence (LA-LIF, also LIBS-LIF) spectroscopy is a large enough body of work to merit its own separate review, LA-LIF and LA-AS are often performed on the same setup and LIF can be considered an indirect (and nonlinear) method of measuring absorption, so a few select fluorescence papers have been discussed in the present review.

Because of the relative complexity and rarity of absorption measurements in the LIP, this review treats the instrumental paradigms for the measurement. The trajectory of uses for LA-AS in the ultraviolet to near-infrared and the main developments that it has generated are also discussed. Because XUV measurements remain uncommon in analytical LIP work, we exclude these from the current review. However, we begin with a brief tutorial overview of absorption measurements and the Beer-Lambert Law.

# 2. Laser-ablation absorption spectroscopy basics

#### 2.1. Requirements of Beer-Lambert Law

Welz and Sperling's excellent book and the references therein provide a thorough review of the complexities of the Beer-Lambert Law and spectral lineshape in the context of flame and furnace-based atomic absorption spectroscopy, with discussion of the resulting potential for artifacts [7]. Although the Beer-Lambert Law is well understood in spectrochemical analysis, the unique properties of the LIP as a reservoir for absorbers call for reconsideration of the demands of the Beer-Lambert Law, namely:

- Monochromatic radiation- i.e. the spectral width of the probe line must be (much) narrower and "purer" than the spectral feature being probed
- 2) All rays must experience the same optical depth
- 3) Plasma optical depth must not change during the measurement's time resolution increment
- 4) Spectral irradiance must not be so high as to depopulate the lower state of the transition

# 2.2. Issue of averaging in Beer's Law and resulting artifacts

The first three requirements of Beer's Law arise from the fact that a given probing averages *transmission* (i.e. the transmitted power)- spectrally, spatially, and temporally. This average is ratioed and logarithmically transformed to (nominally) represent the spatial/spectral/temporal average of *absorbance*. Because transmission and absorbance are only inversely linearly proportional at high transmission- i.e. low absorbance- the averaging can distort the value, over representing the higher transmission portions (rays, wavelengths, times or instances) of the measurements in the calculated "average" absorption. Thus, when a high and low absorption are averaged as *transmissions* or transmitted signal, the subsequently calculated absorbance skews low.

# 2.2.1. Spectral averaging

Achieving the required spectral resolution for demand #1 above is particularly complicated in AAS because of the narrow linewidth of the gas-phase absorbers (see Reference 8 for a thorough discussion of

lineshape in LIPs). Generally speaking, it is common to find linewidths substantially less than 10 pm as the plasma cools, especially at low pressures. While single-mode CW lasers routinely provide linewidths far narrower than such an absorbance profile (stabilization is another issue entirely), achieving this resolution via dispersion of a broadband source, or even with grating-tuned pulsed dye lasers, which may lase on multiple longitudinal modes, is much less trivial. Table 1 provides a summary of typical parameters (or ranges) for probe sources used in LA-AS.

While qualitative measurements of lineshape via absorption strictly require that the width of the slit function be less than that of the spectral line, integrating absorbance peak areas can relax the need for high resolution to an extent in quantitative measurements. To illustrate the impact of instrument function, Fig. 1 presents synthetic data in which a Gaussian absorbance profile,  $k(\lambda)$ , is convolved with a Gaussian instrumental resolution function,  $f(\lambda)$ . Depending on the measurement paradigm, the instrument function is set by either the spectrometer's slit function or the tunable laser's spectral profile. The convolution is not performed directly, rather it is calculated with the transmission (i.e. as f  $(\lambda)*10^{-k(\lambda)}$ ) and the resulting measured transmission profile is then logarithmically transformed to give a measured absorption profile. The ordinate of Fig. 1 gives the ratio of the measured peak area to the original area of  $k(\lambda)$  and the abscissa is the ratio of the widths of the convolved shapes. Gaussian profiles were used here for simplicity of description- actual profiles are likely to be more tail-heavy and the impact of a more "tailed"  $k(\lambda)$  or  $f(\lambda)$  on the data is not straightforward.

The reduction of apparent area in Fig. 1 is minimal at low peak absorbances, no matter the width of the instrument profile. Even this low error becomes constraining for measurements requiring accurate measurements across a large (linear) dynamic range, however. If absorbance is measured at multiple wavelengths and absorber lineshape is known or stable (i.e. can be calibrated away), linearity can be improved by measuring the absorbance signal at a known separation from the peak center, as discussed in Reference 9, though this sacrifices the "absolute" nature of the absorption measurement. For absolute measurements of optical column depth, note that even at an experimentally demanding ratio of instrument/absorber width of 0.5, error is already 10% at a peak absorbance of 1.5.

# 2.2.2. Spatial, temporal and shot-to-shot averaging

Temporal and spatial averaging of the plasma behavior as transmission (i.e. before log transformation) are similarly difficult experimental issues. Plasmas are typically on the order of 1 mm in size at atmospheric pressure. Thus, the probe waist should be substantially smaller than this lest the optical depth vary over the probe cross section and violate demand # 2. Also, the duration of the probe's intraplasma temporal averaging (as determined by detector electronics or the

Table 1
Properties of probe sources.

Probe	Spectral Width	Time resolution
	0.1-400	
Tunable Ti-sapphire laser	MHz	detector-limited
External cavity diode laser (ECDL)	0.5-5 MHz	detector-limited
	0.5 to >5	
Pulsed dye laser	GHz	5 ns
Amplified spontaneous emission (ASE)		
pulsed dye "laser"	~5 THz	10 ns
Type II optical parametric oscillator		
(OPO)	$\sim 100 \text{ GHz}$	5 ns
Frequency comb	>10 THz	1/(spectral resolution)
Xenon flashlamp	>100 THz	>1 μs
Hollow cathode lamp (HCL)	${\sim}2~\text{GHz}$	detector-limited
LIP (line)	10–100 GHz	~μs or detector-limited may require ns detector
LIP (continuum)	>100 THz	gating

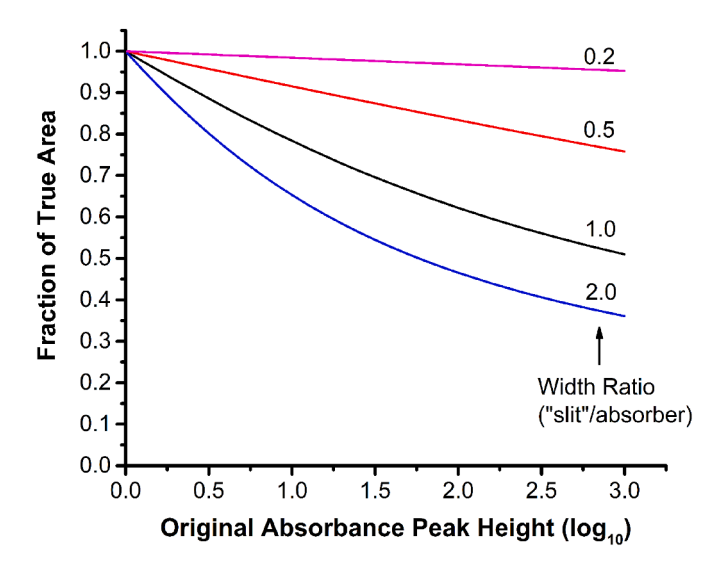


**Fig. 1.** Effect of finite slit width on measured area of absorbance peak as a function of original peak height. Gaussian functions are used for both line profile and instrument "slit" function. The simulation does not consider the effects of stray light or uncorrected plasma emission.

probe's intrinsic duration) needs be substantially shorter than the characteristic time over which the plasma's optical depth varies for analogous reasons. Thus, highly absorbing, transient plasmas must be measured with higher temporal and spatial resolution, as defined by the characteristic time or distance over which the transmitted power (not the absorbance) varies.

LIPs are notoriously irreproducible (despite improvements in lasers) in inhomogeneous matrices, leading to an additional unique consideration when averaging across multiple LIPs to improve signal-to-noise ratio (SNR). If averaging is carried out across a series of ablations, the absorbance must be calculated on the basis of an individual shot, with these individual absorbances averaged subsequently. Averaging the raw transmitted light signals or even  $\rm I/I_0$  in the oscilloscope memory or CCD chip/software leads to overrepresentation of the low-absorbance shots in the absorbance calculated from such previously averaged signals. Once again, this is important at higher absorptions where the fraction absorbed is no longer linearly proportional to the inverse of transmission-lower absorptions relax the requirement.

#### 2.3. Kinetic bleaching

Coherent sources are widely used in LA-AS because they can be tailored to tight beamwaists and long Rayleigh lengths and because they allow very high time resolution in some configurations. However, the experimental advantage of coherent probe sources is limited by their potential to kinetically "bleach" or saturate the transition (violating requirement #4 of the Beer-Lambert Law). Kinetic bleaching results from the fact that the absorption coefficient  $\alpha$  depends on the degeneracy-adjusted difference in lower and upper state populations ( $n_l$ - $n_u$ ) as given by:

$$\alpha(\nu) = \frac{h\nu}{4\pi} B_{lu} \left( n_l - n_u \frac{g_l}{g_u} \right) S_{\nu} \tag{1}$$

where  $B_{lu}$  is the Einstein coefficient for stimulated absorption by the lower level,  $n_l$  and  $n_u$  are the number densities for the lower and upper states, respectively,  $g_l$  and  $g_u$  are their degeneracies and  $S_\nu$  is the normalized lineshape function. As the probe laser's spectral radiance is increased, the rate of stimulated absorption exceeds the rate at which the plasma can relax the population back to unperturbed conditions through collisions or spontaneous emission, resulting in buildup of excited state population and loss of further net absorption as  $n_u g_l/g_u$ 

approaches  $n_l$  and any additional absorption becomes balanced by stimulated emission. This is particularly problematic when using short-pulsed probe lasers, high oscillator-strength transitions, or the narrow beam waists required to fulfill #2 above. Additionally, the low electron and ion+neutral number densities present at the later times and/or reduced pressures popular for reducing linewidths (and likely for increasing plasma dimensions to reduce problems associated with requirement #2) in LA-AAS also reduce collisional relaxation rates, increasing potential for kinetic bleaching of the transition. While working at low absorption decreases the problems associated with the various forms of averaging, only decreased (peak) probe irradiance or working at lower oscillator strengths can reduce kinetic saturation. Though kinetic bleaching is most often encountered with pulsed probes, the effect is by no means limited to them (see, e.g., Reference 10).

# 2.4. Additional sources of artifacts

There are two further experimental consideration beyond the Beer-Lambert Law that bear consideration when working in LIPs. Though not a matter of averaging per se, stray light or uncorrected dark signal has an effect analogous to that of inadequate spectral resolution. Additionally, the LIP is prone to beam steering of the probe which can increase or decrease apparent absorption, resulting in difficult-to-diagnose artifacts.

# 2.4.1. Stray light

The impact of stray light on apparent absorption is discussed by many authors, including References [9] and [11]. As with averaging concerns, stray light is most problematic at high absorbances, hence the use of double monochromators to measure high absorbances in condensed-phase UV–vis spectroscopy. Fig. 2 simulates the impact of varying levels of stray light (assumed to be spectrally flat) on measured peak shape and area. Because the higher-absorbing center of the peak is most affected, the quantitative impact is lessened by the use of peak area. Once again, measurements of peak shape require suppression of stray light and are best made at the lowest absorption giving acceptable signal, where stray light (and finite instrument profile- i.e. spectral averaging) have the least effect.

Thermal probe sources (e.g. flashlamps or secondary LIPs) are

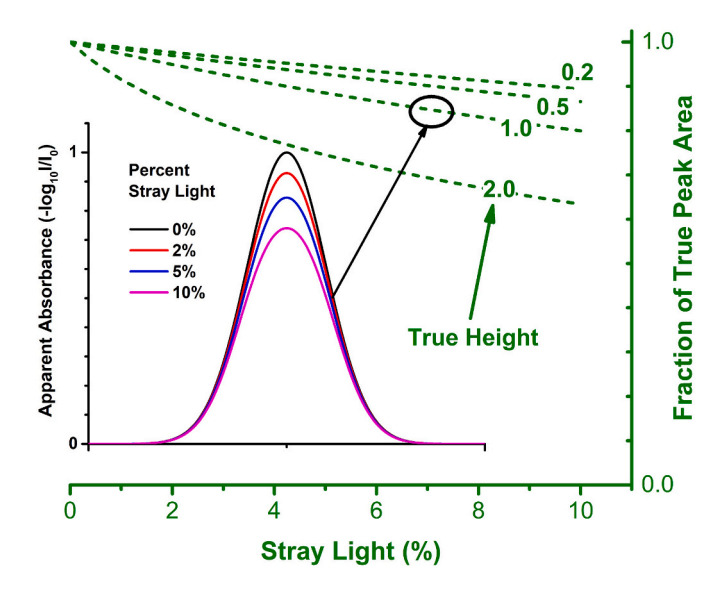


Fig. 2-. Influence of stray light on integrated Gaussian peak area (curves and right scale) and peak shape (inset). For this simulation, stray light is added to both the probe and reference spectrum and is calculated as a fraction of the reference beam at a given wavelength and is assumed to affect all regions of the spectrum equally. The inset show the impact of varying degrees of stray light on the shape of a Gaussian peak of nominal height unity.

limited by the Planck Law and may require subtraction of the thermal emission background emitted by the plasma. Uncorrected, the thermal emission has an effect similar to stray light. When using coherent or semicoherent probes to measure absorbance, the spectral radiance of the probe can easily exceed that of the plasma such that background from the latter becomes negligible at moderate optical depths. The high spectral radiance of (semi)coherent sources is also advantageous when using the low-etendue spectrometers required to generate high resolving power.

#### 2.4.2. Beamsteering

The small size and attendant high spatial gradients of LIPs create significant potential for beamsteering. This can result in either positive or negative signal deviations (depending on the deflection and the optical geometry) and may be a function of wavelength. El-Astal and Morrow have discussed and studied the impact of electron and absorber number density gradients on LA-AS measurements [12]. Because this effect is not otherwise explicitly discussed in the LA-AS literature, I reproduce part of their discussion here.

They remind us that electron number density's  $(n_e)$  impact on refractive index  $(\eta_e)$  is given by:

$$\eta_e(\lambda) \approx 1 - \frac{n_e}{2n_{ec}(\lambda)}$$
(2)

where the critical electron number density, n<sub>ec</sub>, is given by:

$$n_{ec}(\lambda) = \frac{4\pi\varepsilon_0 m_e c^2}{e^2 \lambda^2} \tag{3}$$

Furthermore, close to strong absorption lines, absorber number density  $(n_a)$  affects refractive index as:

$$\eta_a^2(\lambda) \approx 1 + \frac{e^2 f n_a \lambda_0^2 \lambda^2}{4\pi^2 m_e \varepsilon_0 c^2 \left(\lambda^2 - \lambda_0^2\right)} \tag{4}$$

where f is the transition oscillator strength and  $\lambda_0$  the transition's center wavelength. As a result of these physics, probe beams refract *toward* lower electron density in a gradient perpendicular to beam propagation. Similarly, on the red side of strong absorption lines, the probe steers toward the higher absorber number density in gradients number density, and toward lower number density on the blue side. Working at shorter wavelengths and low absorbances can reduce the effects of electron number density or absorber gradients, respectively, but at the cost of experimental flexibility and calibration sensitivity.

# 3. Measurement paradigms

In addition to the usual flicker noise problems of LIBS and the LIP formation process, the above considerations conspire to make LA-AS a challenging measurement, certainly when compared to the (perhaps deceptive) simplicity of LIBS. Over the years, several measurement paradigms have emerged to address these challenges. The implementations vary from elegantly simple to experiments that owe much to recent Nobel prizes. I discuss the details of these paradigms here and note that no one technique dominates the literature. Central to the applications are the source of spectral resolution and the probe light source (these may be the same). I use the latter to organize the discussion and summarize the *approximate* characteristics of the different probe sources in Table 1.

#### 3.1. Atomic-line-source methods

In traditional line-source flame AAS, the necessary spectral purity is effected through the combination of a low-broadening hollow cathode source and a modest resolving power monochromator that isolates the narrow band around the atomic line. Gordillo-Vazquez adapted this to the LIP, measuring hollow cathode lamp (HCL) transmission through the

plume formed by ablation of LiNbO<sub>3</sub> under vacuum [13]. The measurement benefitted from the low ablation energy and vacuum conditions' minimizing the plasma emission and maximizing its dimensions relative to the HCL. However, the HCL's modest spectral radiance limits applications in the LIP. More recently, Moon and Omenetto's duplicating mirror scheme used the plasma's own emission as the probe [14]. They used the LIP's continuum emission (far from the line center) to calibrate the efficiency of duplication, since continuum is not expected to be optically thick. The spectrograph isolated the line and the combination of imaging onto the spectrograph slit and the vertical resolution of the intensified charge-coupled device (ICCD) provided 1-D spatial information in the duplicating mirror measurements. In both the HCL and the duplicating mirror implementations, the ratio of absorption profile to instrument "slit" profile (i.e. the spectral profile of the probe plasma or monochromator slit function, whichever is narrower) was high and potentially poorly known—e.g. Gordillo-Vazquez was forced to assume a LIP spectral linewidth in order to calculate optical depths. Furthermore, the duplicating mirror's use of the LIP as the probe source does add a large source flicker term to the already substantial flicker noise from the LIP being probed. However, the simplicity of the duplicating mirror is undeniable.

#### 3.2. Narrow-line laser probe methods

Despite the added complexity, spectral resolution is more often effected via a narrow-linewidth laser- either a narrowed pulsed laser (e. g. dye) or a tunable CW lasers (dye, diode, etc.). The coherent radiation allows for diffraction-limited focusing at the plasma, albeit with the previously mentioned risk of bleaching the transition. Pulsed lasers allow tight time resolution and access from the deep UV to the NIR, but spectral resolution is often modest. CW lasers provide much more limited spectral access and many wavelengths require complex intracavity harmonic generation, but the linewidths can be exquisitely narrow (see Table 1).

# 3.2.1. Continuous-wave laser measurements

Several groups have implemented LA-AAS with spectrally narrowed CW (continuous wave) probe lasers. In an early and very technical experiment, Niemax' group temperature-current scanned a diode laser several tens of picometers across multiple peaks within a single laser shot [15]. Note that Reference 15 actually detected via fluorescence. Their technique convolved the plasma evolution with the change in wavelength probed, making interpretation of the data difficult. More typically, if measurements are to be made at multiple wavelengths, the laser wavelength is scanned between LIP shots, adding substantial flicker noise. Nonetheless, typical CW probes allow the entire time evolution of the I<sub>transmitted</sub> signal to be recorded on an oscilloscope/fast digitizer within a single shot. These data must be processed carefully, however, to avoid distortion through temporal averaging as transmitted power as discussed earlier.

To suppress the portion of the flicker noise associated with variable beamsteering and particle obscuration, authors have overlapped two CW lasers in the absorbing region- one on-resonance (and scannable between shots) and one off-resonance [16,17]. As Fig. 3 demonstrates, this can be a powerful strategy for improving SNR at low absorbance (noise at high absorbance was not characterized in their experiments). The twin beams can be combined/separated using polarization or via grating. In order take advantage of correlated variation between optical depth at different peaks (i.e. flicker noise in their absorptions), researchers have made spectrally duplexed measurements recording both peaks simultaneously [18]. When demultiplexing is via grating, the angular separation of the two wavelengths puts a lower bound on the probes' mutual wavelength separation, limiting applications. In a simpler variation, Niemax' group has also overlapped two diode laser beams at the plasma while keeping them slightly noncollinear, allowing simple spatial demultiplexing [19].

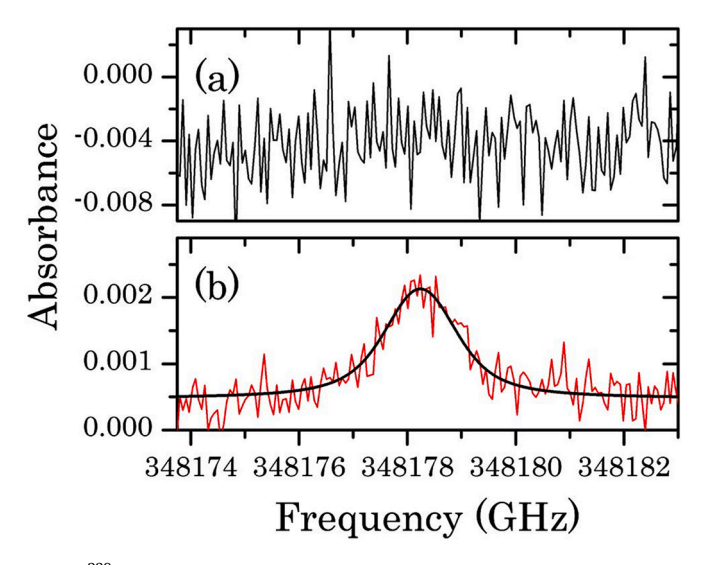


Fig. 3.  $^{238}$ U absorption measured via ECDL with (bottom) and without (top) reference beam normalization. The referencing improves SNR  $8\times$ , bringing measurements within a factor of two of the shot-noise limit. Reproduced from Reference 16.

Lauly has produced a unique implementation of the CW absorption measurement that has not been repeated to this author's knowledge. His resonance shadowgraphy with an external-cavity diode laser (ECDL) probe multiplexed the measurement in two *spatial* dimensions and used the ICCD's photocathode gate to provide temporal resolution. As with other measurements relying on the probe linewidth for resolution, the wavelength was stepped between ablations [20]. This measurement does not take advantage of the time multiplexing allowed by a CW laser, and is only superior to pulsed-dye-laser shadowgraphy in its extremely narrow linewidth. Indeed, Gilgenbach et al. have made analogous measurements with a pulsed dye laser probe and photographic detection with a probe linewidth three orders of magnitude wider than that of Lauly (5 MHz), as is typical of pulsed lasers [21,22]. Given Gilgenbach et alia's use of photographic film detection and modest laser narrowing, it is understandable that their studies were largely qualitative.

### 3.2.2. Pulsed laser measurements including cavity ringdown spectroscopy

Overall, pulsed (spectrally narrow, tunable) probe laser measurements are surprisingly uncommon in LA-AS given these lasers' flexibility and their previous use in LA-LIF measurements. Duffey et al. generated (laboriously wavelength-scanned) maps of absorption depth using a scanned dye laser in excimer ablation plasmas [23]. Such twodimensional measurements are uncommon, perhaps because of the labor involved. Researchers at Queen's University (Belfast) have produced a series of papers probing the LIP with pulsed dye lasers [12,24–28]. They incorporate photodiode array detection to multiplex their absorption measurements with resolution in a single spatial dimension. As this requires illumination with a probe laser sheet, they also incorporate simultaneous measurement of fluorescence tomographic images via ICCD [25]. The fluorescence data are complicated to interpret, however, unless the optical depth is extremely low. In all of these pulsed measurements, inter-ablation scanning of the probe laser (incorporating flicker noise in plasma transmission) is required to generate absorption spectra and the plasma-probe delay must be scanned from shot-to-shot.

The group at the Institute of Physics in Zagreb has produced an interesting variation on the pulsed laser measurement, combining a dyelaser probe with cavity ringdown spectroscopy (CRDS). Experimentally, the long ringdown time allows ablation and probe dye-laser pumping with the same excimer laser. Generally, the CRDS measurement has the benefit of being self-normalizing- i.e. it reduces *source* flicker noise if a

full ringdown is recorded with every shot. Flicker noise in the plasma's optical depth remains, however, since data are typically averaged, and the wavelength scanned across multiple ablation events. The plasma's small size relative to most cavities means that only part of the benefit of the CRDS measurement is realized, even when working with the large plasmas generated at low pressures. Furthermore, CRD should not be thought of as *extending* the linear dynamic range to lower absorbances so much as shifting the linear dynamic range lower, as the loss of linearity (rollover) can be expected to occur at a lower absorption.

In applying CRDS to the LIP, interpretation of the ringdown is complicated by the fact that the plasma evolves on approximately the same timescale as the cavity's signal decays, resulting in multislope ringdown traces (see Fig. 4), in which the ringdown time becomes a function of time. The dynamic nature of the plasma puts a further limitation on the sensitivity benefit of CRDS since the empty cavity ringdown time ( $\tau_0 = L/[c^*(1-R)]$ ), where R is cavity reflectivity and L is cavity length) must be kept shorter than the characteristic time over which the plasma evolves by using a short cavity and low mirror reflectivity. Practically, there is a lower limit set on improvements to time resolution generated by decreasing cavity length- eventually the mirror fouling with ablation products becomes unacceptable.

# 3.3. Continuum source probe methodology

Continuum-source AS (CS-AS) has been used by a small number of

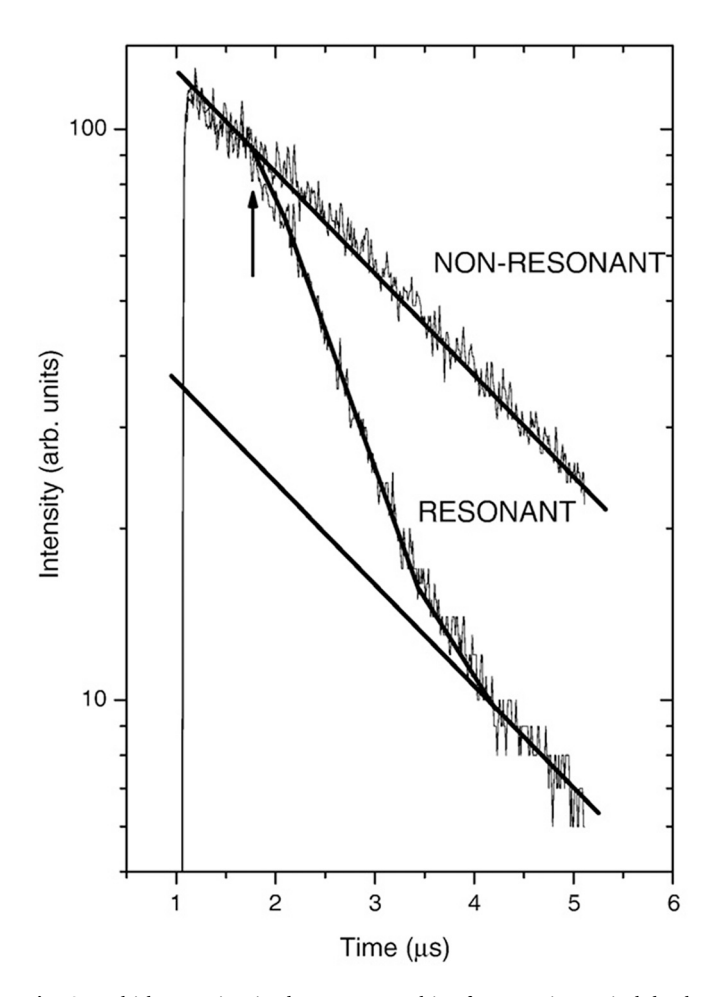


Fig. 4. Multislope cavity ringdown trace resulting from varying optical depth as the plasma evolves. Note the arrival of absorbers at  $\sim 2$  microseconds (arrow) where the resonant and non-resonant curves diverge. The resonant trace is recorded with the laser tuned to the titanium transition at 625.88 nm. Reproduced from Reference 29.

LIP research groups over the years. CS-AS monochromates (polychromates, more typically) a relatively broadband probe source (a semicoherent laser-like source, frequency comb, or plasma blackbody) post-sample to satisfy the requirements of the Beer-Lambert Law. CS-AS (mostly CS-AAS) has a long history and is commercialized for flame and graphite-furnace atomic and molecular measurements, with in-depth discussion in Reference 9 and the references therein. Of course, the flame and graphite furnace are both much larger and much less dynamic than the LIP, simplifying the measurement relative to the latter.

In general, CS-AAS measurements in the LIP can be thought of as a highly multiplexed version of the spectrally duplexed diode laser measurements, with the demultiplexing now achieved with a high-resolution spectrograph to form an entire spectrum with each plasma probing. Because the peak and baseline are measured simultaneously, flicker noise caused by variable beamsteering or particle obscuration propagates as an easily subtracted offset in the flat background. Similarly, if the continuum probe is spectrally flat at the level of the absorption feature, flicker noise in the *probe intensity* also propagates as an easily subtracted baseline offset. Of course, when there is substantial mismatch between the probe spectral width and the width of a given absorber, the stray light may become significant, reducing calibration sensitivity, and shifting the onset of sublinearity to lower absorbances.

# 3.3.1. Laser-induced-plasma continuum probe source methods

Several broadband probe sources have been used for LIP absorption. The simplest method applies to situations with grossly self-reversed lines, or "Fraunhofer" absorption of plasma continuum from the plasma center by cooler atoms at its periphery as seen in Fig. 5. Nagli and Gornushkin used a collinear dual-pulse arrangement to backlight a cooling plasma with continuum emission using a probe plasma subsequently generated at the center of the previous plasma [31,32]. Their experiments required tight gating around the probe plasma initiation, with the ICCD gate width kept between 7 and 10 ns to select for the broadband portion of the probe's emission. Ribiere et-alia's dual-ablation designs used adjacent probe and reservoir plasmas (see Fig. 6) [30,33]. Cui et al. have recently used the concentric-plasma geometry for measurements underwater [34,35]. Plasma continuum light sources are particularly suited for the vacuum and deep UV, where light sources are problematic (XUV and soft x-ray experiments are not

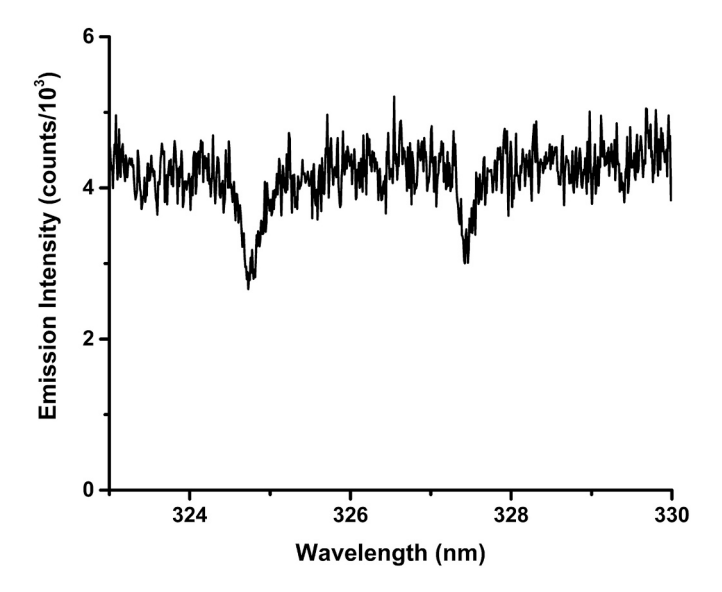


**Fig. 5.** "Fraunhofer" absorption of plasma continuum emission by copper resonance transitions in the first  $\sim 5$  ns of a 500 ps powerchip laser-induced plasma formed on brass. The spectrum was recorded with a 0.5 m Czerny-Turner spectrograph with a 2400 mm $^{-1}$  grating and an unknown slit width and appears to either underresolve the absorption or to suffer from stray light. Author's unpublished work in the laboratory of N. Omenetto.

considered in this review for the sake of brevity, but their use in atomic physics is covered extensively in the review by Costello et al. [3]). In contrast to measurements made with (semi)coherent sources, the probe optical path is somewhat poorly defined with dual-plasma arrangements and may violate the requirements of the Beer-Lambert Law to an extent.

#### 3.3.2. Flashlamp probe source measurements

The researchers at Queens University, Glumac's group (University of Illinois) and Geohegan and Puretzky (Oak Ridge National Laboratory, USA) have used xenon flashlamp plasmas imaged through the LIP to measure absorption [36-40]. Although these probes have been used for atomic measurements, they are particularly suited to molecular absorption studies, where it can be desirable to make simultaneous measurements over several nanometers to record an entire molecular progression. Taking this broad bandwidth measurement to the extreme, Geohegan et al. have even used flashlamps to measure the absorption of matrix-assisted laser-desorption ionization (MALDI) matrix plumes after ablation [41,42]. In more typical ablation measurements, if absorption is sought sufficiently early in a vigorous LIP's development, the radiance of the probe and LIP can be similar, requiring subtraction of a plasma emission signal and adding another noise term. These probes have durations that can vary with wavelength and that are on the same order as the LIP, so detector gating is necessary to generate time resolution better than ~1 µs [40]. Additionally, Weerakkody and Glumac point out that their Xe discharge plasma is  $\sim$ 4  $\times$  2.5 mm, larger than most atmospheric pressure LIPs, which along with the long measurement time (with ungated detection) limits linearity and potential for absolute measurements. In theory, it is possible to aperture the discharge plasma, which would allow improved spatial resolution and attendant improvement to sensitivity and linearity. In fact, the spectrometer slit width already apertures the probe source in one dimension. Nonetheless, the authors achieve extremely high SNR in the low-absorption limit.

# 3.3.3. Semicoherent probe source (pseudocontinuum) methods

Glumac and Merten have also used semicoherent, pulsed continuum probes, which Merten refers to as pseudocontinua. These have included amplified stimulated emission (ASE) from a dye cell, frequency-doubled ASE from dye cells, and a type II optical parametric oscillator (OPO) (see Table 1) [43-46]. Glumac's measurements with the (doubled) ASE probe were actually in transient fireballs ignited by exploding bridgewires, where single-shot measurement capabilities are essential, but the technique should also be applicable to LIPs. Merten and Johnson have found nanosecond OPO spectra to be quite structured (see Fig. 7) at the single-picometer level relevant to cooled atomic absorption peaks, making a dual-beam-in-space arrangement essential to suppress the source flicker noise caused by shot-to-shot variation in the probe's spectral structure. Unlike plasma continuum probe sources, these semicoherent probes are easily focused to small (~100 μm) waists with long Rayleigh ranges which minimizes spatial averaging across different ray trajectories and clearly defines the probe geometry.

# 3.3.4. Further experimental considerations in continuum-source methods

No matter the exact probe, continuum-source absorption measurements rely on the spectrograph to meet the monochromaticity requirement of the Beer-Lambert Law. As such, most of the continuum-source methods use long focal-length (>1 m) grating spectrographs, with simultaneous inspection ranges inversely proportional to resolution. Welz et al. point out that relative shot noise in a given pixel also increases with the square root of resolving power, decreasing the SNR [9] though the relevance of shot noise is quite complicated in LA-CS-AS measurements- both Glumac and Merten found that shot noise was not limiting at low absorbances in the case of single-beam measurements (see, e.g. Fig. 7) [43,45]. Merten has resorted to extremely high monochromator resolving powers (>10<sup>6</sup>) to resolve the structure of the OPO spectrum in attempts to reference away flicker noise at low absorbances using dual-beam data processing (see Fig. 7). Because the semicoherent

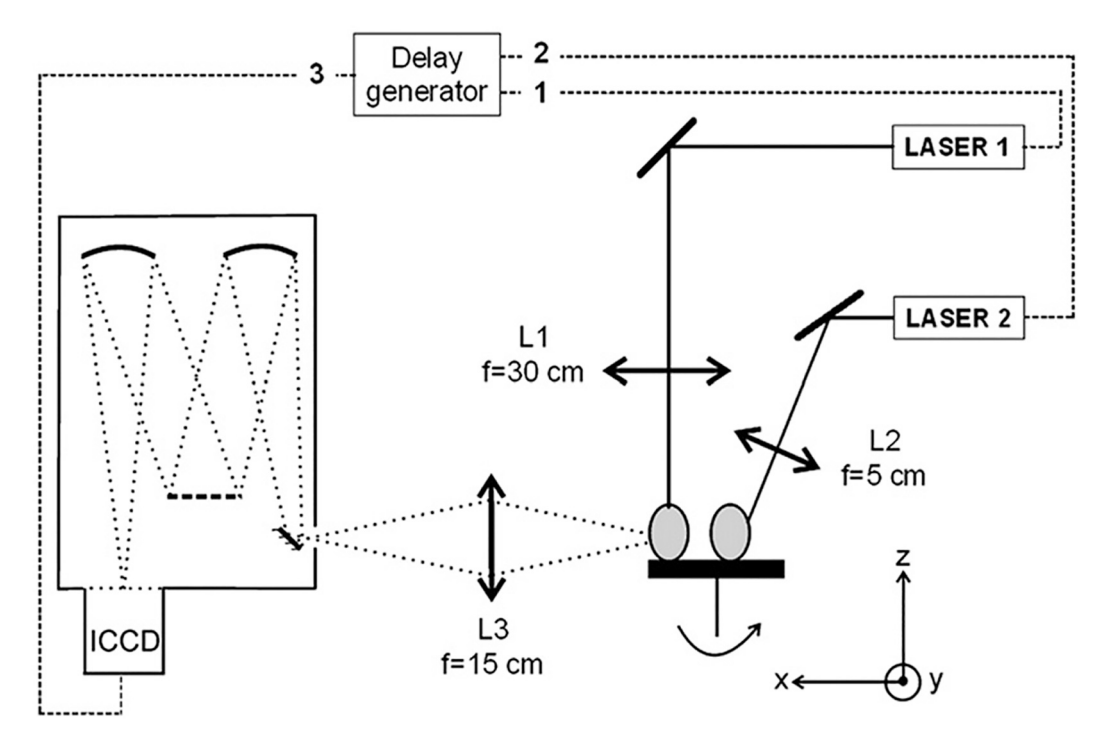


Fig. 6-. Dual-plasma continuum-source arrangement using adjacent-plasma geometry. Reproduced from Reference 30. More recent experiments use a concentric-plasma geometry.

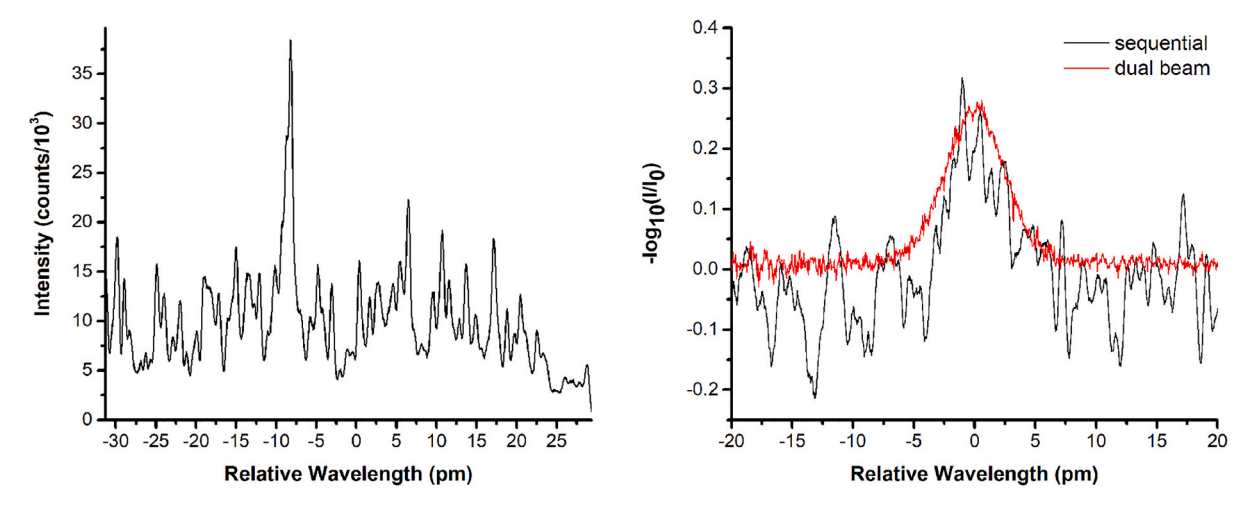


Fig. 7. Irregular structure of type II OPO at high resolution (L). Dual-beam-in-space measurements (R, red trace) are required to remove noise that would otherwise remain in absorption spectrum (R, black trace) as a result of variation in the probe's spectral structure. Adapted from Reference 45. (For interpretation of the references to colour in this figure legend, the reader is referred to the web version of this article.)

probes are not extended sources, it is relatively simple to produce high throughput at the spectrometer, even with extremely high resolving powers. In fact, Merten and Johnson have capitalized on the low divergence of their OPO probe source to build a unique 2-m, double-pass echelle spectrograph that uses cylindrical rather than spherical optics and allows simultaneous measurement of probe and reference spectra on a 2D detector face. Pairing this spectrometer with a narrow OPO "pseudocontinuum" obviates order sorting, which would otherwise demand spherical optics and a second dimension of dispersion, complicating the dual-beam arrangement.

#### 3.3.5. Dual-comb spectroscopy

Extremely broadband dual-comb spectroscopy (DCS) absorbance measurements have recently been demonstrated in the LIP [47–51].

Dual comb measurements are discussed by Swann and coworkers, but I provide an outline of the technique here [52,53]. In contrast to other "continuum" probe methods, DCS does not require monochromation after the plasma per se. DCS can be understood through analogy with Fourier-transform interferometry (FTIR). Two frequency combs (typically femtosecond lasers) operating on slightly different repetition frequencies ( $f_{\rm rep1} \neq f_{\rm rep2}$ ) but with a  $\sim$  fixed phase relation are allowed to interfere at a common detector thereby recording the interferogram. In analogy to FTIR, the scan by stepping the position of the variable interferometer arm is replaced by the inherent step in relative phase between the combs from pulse to pulse as a result of  $\Delta f_{\rm rep}$ . An entire interferogram is collected extremely rapidly— every  $1/\Delta f_{\rm rep}$  with the probes' optical frequencies now shifted radiofrequency beatnotes. The interferograms can be added coherently (within the limits imposed by

the combs' mutual coherence time) to improve figures of merit if a consistent phase relation is maintained between the two combs via a transfer oscillator (e.g. a stabilized or slowly-drifting CW laser).

Like the other wavelength-multiplexed measurements, DCS has the benefit of removing much of the plasma's shot-to-shot flicker noise in nonresonant losses, which only create an easily subtracted baseline offset. However, shot-to-shot coaddition of interferograms to improve SNR requires careful phase locking between the loops to keep the mutual coherence time longer than the period over which shots are coadded. Note that if optical depths are high and vary from shot to shot, coaddition of subsequent transients (without first calculating absorbance) will skew apparent absorption measurements low as discussed earlier. Additionally, at the typical  $\Delta f_{rep}$  of a few hundred Hz, the entire interferogram requires on the order of a millisecond, which would convolve measurements with the plasma's temporal evolution in most cases. As a result, truncated acquisitions of the interferogram are used, which decreases spectral resolution. For example, Jones' group used a 440  $\mu s$ acquisition time at  $\Delta f_{\text{rep}} = 520 \text{ Hz}$  to achieve a spectral resolution of 0.53 GHz (1 pm) in the NIR region sampled with doubled Ti:sapphire combs [47]. This was sufficient to resolve the hyperfine splitting of the rubidium D lines while simultaneously measuring the potassium D lines 6 THz away (see Fig. 8). They also report measurements in a band around ~530 nm produced with doubled Yb-fiber frequency combs operating at 78 MHz [49]. Here, acquisition of a 20 µs interferogram achieved a resolution of 8 GHz (8 pm) at a  $\Delta f_{\text{rep}}$  of 510 Hz.

Dual comb spectroscopy stands apart in its ability to measure large spectral ranges with high resolution in a single ablation event, but certainly has limitations. When probing with a flashlamp continuum, the spectrometer imposes a tradeoff between resolution (and thereby linearity) and simultaneous observation range. In DCS, the analogous tradeoff is between spectral and temporal resolution, both of which are important to the technique's linearity. As a result, measurements to date have focused on low-pressure, late-stage, semi-stationary LIPs. As with other FT spectral methods, DCS incurs a multiplex *disadvantage* as larger spectral ranges are measured simultaneously, so the comb may be spectrally narrowed with a filter or grating to select a more limited spectral region of interest. Additional multiplexing is possible- Jones' group has recently demonstrated "burst mode" DCS of LIPs, measuring a

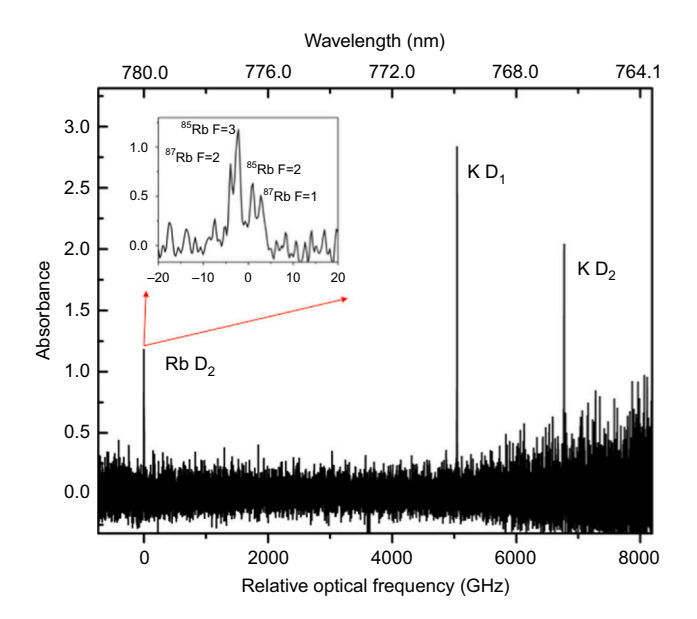


**Fig. 8.** Single-shot absorption DCS spectrum in a LIP. Absence of the expected 2:1 height ratio of the potassium D lines suggests potential sublinearity at this high absorbance or may be the result of noise or aliasing in the figure's generation. The authors use the natural log definition. Reproduced from Reference [47].

 $\sim 500$  GHz spectrum at eight different delays within a single ablation [54].

# 4. Applications of laser-ablation absorption spectroscopy

That researchers are willing to bend a technique like dual-comb spectroscopy to LA-AS speaks to the interest in applications of laser ablation. For example, LIPs have great promise for rapid, sample-prep free analysis as LIBS. Understanding matrix effects and the plasma evolution, however, is critical and may benefit from LA-AS studies. Much of the original development of LA-AS was driven by the development of pulsed laser deposition (PLD) for the manufacture of novel materials, particularly high-temperature superconducting rare-earth barium-copper oxides (REBCOs). Understanding ablation physics, plasma dynamics and chemistry is important for development of this technology. Nuclear power and nuclear weapons manufacture and safety also stand to benefit from LA-AS, both through its potential for rapid analysis of isotope ratios as well as understanding the dynamics and chemistry of LIPs as a simulant for nuclear detonations. Finally, a few fundamental analytical chemical measurements have been attempted with LA-AS. To organize discussion of the results, I have tried to roughly divide research by the authors motivation, or at least the implications of their conclusions. Of course, many papers include multiple thrusts, and the interpretation of authors' intentions and the significance of their results is subjective.

# 4.1. Isotope analysis

LA methods are of interest for rapid, matrix-independent measurements of isotope ratios. This is possible because the isotope shifts between many isotopes of interest ( $^{235}$ U/ $^{238}$ U,  $^{6}$ Li/ $^{7}$ Li,  $^{239}$ Pu/ $^{240}$ Pu) are adequate to spectroscopically resolve the isotopes at some atomic transitions. Isotope shifts in lighter elements are driven by the shift in the atom's center of mass into the nucleus with increasing atomic number (mass isotope effect), while isotope shifts in heavier elements are the result of the field isotope effect, whereby changes in mass number change the distribution of charge in the nucleus, perturbing energy levels. Isotopically resolved measurements have been made with LIBS (i.e. thermal emission) in the past, but the experiment is complicated by the ~inverse relationship between signal intensity and selectivity since the isotope shifts are less than 25 pm. LA-AS, on the other hand, works best at long delays, where the ASDF has collapsed down to a few low-lying and metastable states and broadening is decreased. Although interest is mainly in uranium and plutonium isotope measurements, other elements, including rubidium [8,10,47], cerium [55,56], gadolinium [18,57] and lithium [45,58] have been used as testbeds. I do note that measurements of lithium isotope ratios are themselves relevant to some molten salt reactor and thermonuclear weapon designs.

Despite Niemax's and Winefordner's groups' having first used LA-AAS for isotopic measurements in 1999, selectivity and linear dynamic range remain problematic [10,15]. The combination of finite linewidths, (hyper)fine structure and modest isotope shifts makes selectivity challenging. For example, the greatest shift measured to date in uranium, the U (II) 424.437 nm transition has an isotope shift ( $^{235}$ U –  $^{238}$ U) of only 25 pm. As the linewidth (and potentially its Stark-shifted position) evolves, the extent of the interference changes, making a simple offset correction difficult, particularly if linewidth is not known (i.e. if entire spectra are not recorded). In situations requiring measurement of relatively extreme isotope ratios (e.g. natural uranium containing <1%  $^{235}$ U), the limited linear dynamic range of absorbance measurements restricts applications.

# 4.1.1. Transition linewidth

Measuring and fitting entire spectra can improve selectivity when measuring extreme isotope ratios. For example, Miyabe et al. have produced the only LA-AAS works with plutonium to date, studying <sup>239</sup>Pu and <sup>240</sup>Pu in mixed-oxide (MOX) pellets under 800 Pa of helium and with a selection of ECDLs [59]. When only the peak wavelengths were measured with intershot wavelength scanning, the more abundant peak contaminated signal at the less-abundant isotope in a time-dependent manner as the linewidths evolved. This was correctable with only one wavelength measured per isotope but requires a reproducible variation of linewidth with time. Acquisition and fits of entire spectra obviated the correction but required longer acquisitions and greater sample consumption. Better control of spectral widths would allow improved selectivity without recording entire spectra.

Largely because of its impact on isotopic selectivity, much effort has gone into understanding and controlling linewidths. Of course, this also serves as an important plasma diagnostic. For a thorough discussion of linewidth considerations, the reader is referred to Harilal et al.'s review of LA-isotope measurements [6].

Despite the its high atomic mass, Gornushkin et al. found that, between 1 and 10  $\mu s$ , Doppler broadening dominated minor component (Rb) linewidths under 0.1–10 Torr of Ar, while resonance broadening dominated matrix-derived lines [8]. Taylor and Phillips studied the width of the 861 nm transition of uranium as a function of dry air pressure at a fixed time (7  $\mu s$ ) and position [16]. The Gaussian width was independent of pressure at 1 GHz (2.5 pm). The Lorentzian contribution surpassed the Gaussian width at  $\sim\!500$  Torr, though the two remained similar all the way to one atmosphere.

Harilal et al. have studied linewidth of the aluminum 394.4 nm transition as a function of argon cover pressure and delay after femtosecond laser ablation [60]. They found that linewidth decay was fastest for higher pressures, though the asymptotic value increased with pressure. Working at a single line-of-sight, Harilal et al. have found femtosecond plasmas to provide a superior combination of narrow absorption linewidth and high optical depth relative to nanosecond ablation at the same fluence [61]. Though linewidth generally decreases with pressure, Bushaw and Alexander, Milosevic's group, and Miyabe et al. found that sufficiently low-pressure ablation of strontium, titanium, iron and cerium resulted in a symmetrical Doppler splitting of lines at certain delays, with obvious implications for linewidth [55,62-64]. Fig. 9 illustrates the origin of the splitting with high-resolution ECDL fluorescence images of gadolinium plasmas. In an effort to extend lithium isotope measurements to atmospheric pressure, Hull et al. attempted a dual-pulse ablation with ECDL scanning inter-shot, under the premise that this should reduce linewidths [58]. Though the additional pulse may have reduced linewidths slightly, this was at the expense of greatly increased flicker noise.

# 4.1.2. Linear dynamic range- noise and linearity

On the low absorbance side, measurement LDR is determined by a combination of flicker noise in reservoir transmission (including beamsteering), noise in reservoir emission, detector/amplifier noise, and source flicker and shot noise (though one is typically dominant) and varies with the measurement paradigm and plasma conditions. At high absorbances, linear dynamic range in absorption spectroscopy is limited by stray light and the finite degree of violation of the first three

assumptions of Beer's Law. These combine to cause a flattening of the apparent absorbance response at high optical depth. As such, the push for linear dynamic range in isotope measurements is aided by the low pressures often used to improve selectivity and sensitivity via decreased linewidths. These lower pressures increase the plasma dimensions, decrease the gradients and rate of evolution, and may make the plasma morphology more reproducible from shot to shot, all of which decrease "averaging" concerns and may also decrease flicker noise in the optical depth and beamsteering.

However, reduced pressure alone does not seem adequate to yield acceptable dynamic range. To this end, Liu et al. duplexed their measurements, probing the minor isotope at the peak center and measuring the major isotope in its wings in an attempt to extend linear dynamic range [19]. Reproducibility was unsatisfying and they opted to measure the more abundant <sup>238</sup>U absorption out of an excited state (4421 cm<sup>-1</sup>) and the less abundant <sup>235</sup>U from the ground state (gf values were similar for the transitions). This was successful but requires a calibration curve and reproducible evolution of temperature, line broadening, and line position—all of which may be acceptable for many applications. Nonetheless, they used the calibration from U<sub>3</sub>O<sub>8</sub> pellets to measure natural pitchblende with reasonable success. In contrast, Smith et al.'s intra-pulse-scanned fluorescence measurements solved the problem by scanning from the low to high-abundance peak as the optical depth decreased in the course of plasma evolution [15]. This measurement requires a calibration curve and matrix-matching of plasma evolution and persistence. Repeating Liu et alia's attempt at extended linear range via off-peak measurements to CS-AAS or DCS-AAS would remove the uncertainty in wavelength position that likely limited their precision but would still require reproducible lineshape and therefore matrix-matched calibration. Even in CS-AS measurements, any variability in lineshape would lead to additional loss of precision over measurements at peak centers.

At the low-absorbance extreme, wavelength-duplexed and multiplexed schemes may improve SNR and limit of detection (LOD) by suppressing correlated flicker noise. Taylor and Phillips calculate that their differential-absorption diode laser measurement is within a factor of two of the shot-noise limit [16]. Hull et al. have suggested using this differential setup in their dual pulse measurements to achieve the decreased linewidths of their double-pulse measurement without the added flicker noise [58].

Though duplexing/multiplexing is beneficial for low-signal SNR, the first duplexed absorption measurement was made by Bushaw and Anheier in a scheme that allowed *single-shot* isotope ratio determinations in microscopic particles of gadolinium- a significant achievement in both SNR and linear dynamic range [18]. By probing the isotopes at different transitions originating from different levels of the ground term (and therefore different degeneracies) they were able to reduce the effect of nonlinearity without introducing substantial temperature dependence since the lower levels were only separated by  $\sim\!200~{\rm cm}^{-1}.$  The measurement simulated detecting highly enriched uranium particles in a background of natural or low-enriched uranium.

Though Taylor and Phillips' was a signal + background duplexing, simultaneous measurement of both isotope peaks and background (i.e.

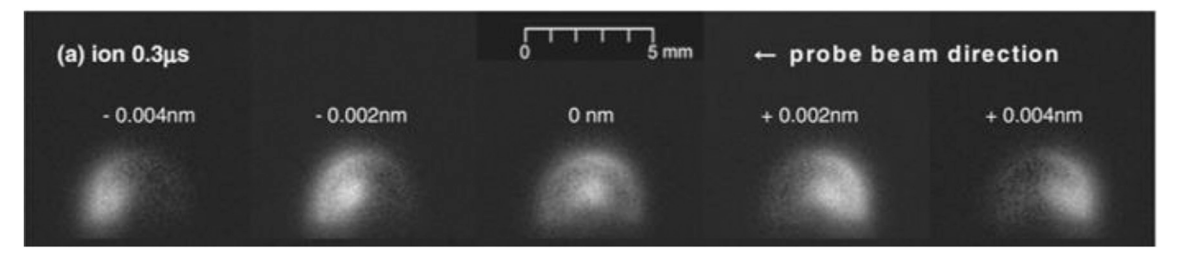


Fig. 9. Fluorescence image of gadolinium plasma at different excitation laser detunings demonstrating splitting of the ablated material into different Doppler populations by the radially symmetrical expansion. The probe laser is incident from the right. Reproduced from Reference [65].

CS-AAS) has potential to improve measurements further, though the CS-AAS and DCS proponents have yet to make close measurements of their limiting noise. CS-AAS should improve correlation between the isotopes' optical densities at intermediate absorbances as well, at least relative to measurements with a single diode laser scanned between shots. CS-AAS measurements in graphite furnaces use off-peak measurements to extend linear dynamic range, a benefit that might extend to LA-AS.

Fluorescence is generally considered to provide lower LODs than absorption spectroscopy and might be expected to benefit isotope ratio measurements. For example, Harilal et al. use tunable diode-laser-excited fluorescence to measure uranium isotopes at the 713.08 and 763.38 nm absorption lines [66]. They point out, however, that fluorescence signal ( $S_{\rm F}$ ) is inherently nonlinear because it is proportional to the absorbed power (or energy in pulsed excitation measurements) rather than absorbance, i.e.:

$$S_F(\lambda_{ex}, t) = S_0 I_0 \left[ 1 - e^{-A(\lambda_x, t)} \right]$$

$$(5)$$

where  $I_0$  is the incident excitation power,  $S_0$  is a constant describing various efficiencies and  $A(\lambda_{x}\text{,}t)$  is the absorbance. The absorbed fraction (the term in square brackets) is only linearly proportional to absorbance in the limit of low absorbance. The authors note that although the LOD for the less abundant isotope may be lower with fluorescence, the earlier loss of linearity in the more abundant isotope offsets the improvement somewhat. They conclude that absorption may be superior given its fundamental linearity (though linearity of absorption measurements at high absorbances is limited by the effects discussed in Section 2). Like Miyabe, the authors also found that measured isotope ratios were a function of delay after ablation, with measurements at later times approaching the expected isotope ratio. Unlike Miyabe, they conclude that this is the result of a loss of linearity rather than selectivity issues. The difficulties of LA-AAS measurements at high absorbances are only vaguely discussed in the literature, but with appropriate attention to electronic bandwidth, probe diameter at the plasma, and any background emission by the plasma, ECDL measurements may be the paradigm best suited to high absorbance measurements.

# 4.2. Plasma diagnostics

# 4.2.1. Pulsed-laser deposition plasma characterization

Relative to isotope ratio measurements, characterization of PLD plasmas by LA is perhaps a less challenging problem. Though easier than the absorption measurement, characterization of plasmas under pulsed laser deposition conditions by thermal emission spectroscopy methods is fraught- the likely athermal nature of the reservoir complicates interpretation of data and much of the plume is present as "dark" metastable and ground state species. Ion probe measurements, on the other hand, have limited selectivity. Nonetheless, control of the kinetic distribution of ablated material is important to the properties of the deposited material: high kinetic energies in the incident plume can damage the growing film, while sufficiently dense plumes of lower energy material may condense en-route to the substrate and deposit as film-contaminating particulates. Thus, control of number density and material flux is also desirable.

The kinetic energy of the PLD plume is commonly derived from time-of-flight measurements or fits of absorption lineshapes at a fixed time. Among the former, Cheung et al. used a CW dye laser probe to measure absorption as a function of time after ablation of YBCO substrates with 532 nm [67]. The times-of-flight of Ba, Ba<sup>+</sup>, Y and Cu number densities were fit, with low fluence ion data conforming to a one-component velocity distribution and higher fluences requiring a two-component Gaussian distribution of velocities. Neutral distributions showed lower kinetic energy and conformed to a single Gaussian velocity component. Note that equivalent information can be had from studies of the absorption *lineshapes*, as demonstrated by Krstulovic et al. with their cavity-ringdown setup [29].

In their flashlamp-probed experiments, Geohegan and Puretzky have studied the ablation plume's splitting into a two-component velocity distribution. They found that the high-velocity component has a velocity approximately equal to that observed under high vacuum and that this component disappears at greater distances from the surface [38,68]. Their modeling efforts indicated that this faster (up to 250 eV) component was due to unscattered penetration of part of the plume into the background gas when the mean free path was similar to the distance at which TOF is measured [69]. The lower-speed scattered particles were readily observed in emission while the high speed component were not.

Given interest in protecting the film from the effects of higher speed particles, Biscan and Milosevic studied the *backscattered* component via lineshapes extracted from wavelength scans in their CRDS setup. The backscattered atoms showed a lower integrated flux (10%) and speeds (3.3 vs.  $8.7 \times 10^3$  m/s) relative to the forward scattered material. The same authors also studied the production of helium metastable under PLD conditions [70]. They found that the He\* was thermalized (relative to the more beam-like propagation of ablated material) and concluded that it originated from collisions with electrons and target atoms previously raised to highly energetic states during the ablation pulse.

The chemistry of material transfer in PLD is also important and has been studied by LA-AS, with substantial contribution from molecular absorption spectroscopy. In a study of nanocrystalline NbAl3 formation following laser-ablation under low-pressure helium, Duffey et al. calculated absolute masses of niobium ablated using atomic absorption imaging and compared these to measured mass removal rates [23]. The comparison provided evidence of either substantial ablation as niobiumcontaining molecules or the rapid reformation of such molecules before the probe laser delay. In their studies of YBCO ablation, Sakeek et al. found that lower laser fluence (<6 J/cm<sup>2</sup>) led to substantial vaporization of target as molecular YO [24]. On the same setup, Morrow et al. showed that a cloud of thermalized molecular material persisted for up to a millisecond under ~100 mTorr of oxygen and speculate that this may be the source of observed off-axis deposition and should generally create an overcoat of molecularly-derived species [37]. Persistence to such long delays was not observable in emission. They calculate the number densities of YO, atomic yttrium and atomic barium when ablating under ~200 mTorr of oxygen, finding that over 95% of the ablated atoms Y and Ba have been converted to molecular oxide species before they reach the target, but that the Cu remains unreacted, presumably oxidizing after deposition [39]. In their study, molecular absorption and emission spectra were quite distinct; the emission spectra were higher-temperature, presumably because they were vibrationally unthermalized chemiluminescence (see Fig. 10).

In studies under low pressures of H2 gas, Labazan et al. found that focusing their XeCl laser slightly above their graphite target yielded more C<sub>2</sub> than the more usual situation of focusing at or below the target. They speculate that the increased laser-plume interaction when the laser was focused in the developing plume further fragmented more of the ablated polyatomic C<sub>n</sub> molecules to form the diatomic. In their measurements of Li2, Na2, K2 and LiNa molecules following ablation of the pure metals and alloy, Labazan and Milosevic found low rovibrational temperatures (50-200 K). Because molecules formed in the plume would be expected to thermalize at a higher temperature, they conclude (like Sakeek et al.) that the observed diatomics are primary ablated particles [71]. They also found that adding a low-pressure He atmosphere reduced dimer production relative to vacuum conditions. Working at turbomolecular pump pressures, Tarallo et al. ablated BaH2 to study production of BaH plumes for molecular cooling and trapping studies [72]. They used a CW diode probe and time-of-flight measurements and discovered that poor thermal conduction in their sample and high ablation repetition rates resulted in thermal desorption from the target as repeated ablations heated it.

# 4.2.2. Nuclear fallout simulations

Modeling the chemical processes occurring in nuclear fallout

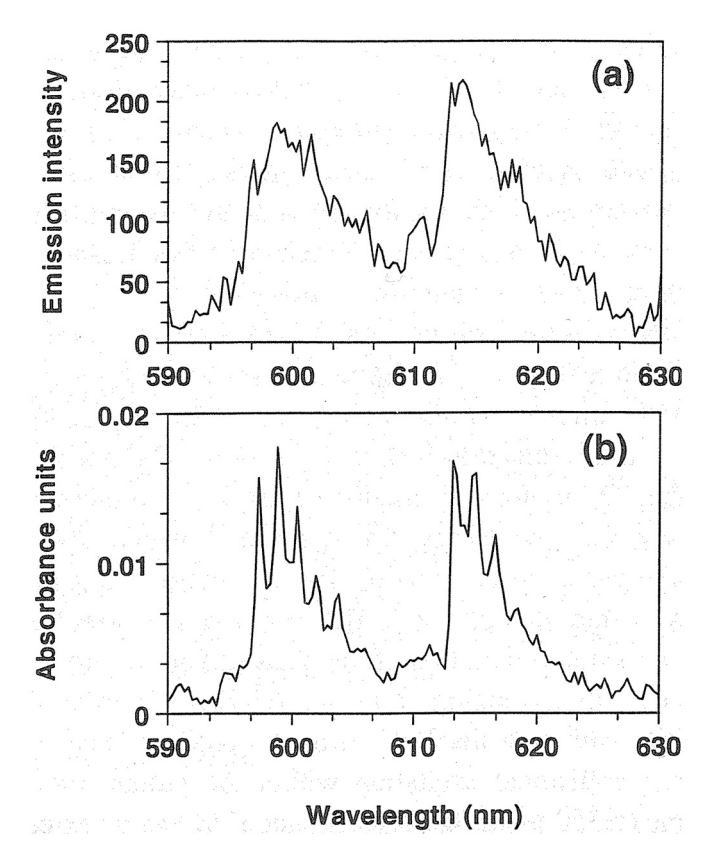


**Fig. 10.** Comparison of thermal emission and absorption spectra of YO upon ablation of YBCO under 300 mTorr of oxygen. Figure reproduced from Reference 39.

requires detailed understanding of the concentration and temperature gradients in the explosion. The LIP presents a uniquely accessible simulation of aspects of this complex process. The role of the surrounding gas in plume chemistry is presumably important to development of both nuclear fallout and production of particles after ablation. Given the interest in modeling fallout, Weerakkody and colleagues have recently returned to flashlamp continuum probes for measurements in cooling LIBS plasmas [36,40]. Though the work is mostly proof of concept, they have demonstrated measurements of SiO, BeH, UO, and ZrN absorbance bands (at absorbances < 0.01 in many cases) in addition to atomic and ionic line absorbance. Many of the molecules demonstrated are the result of reactions with the ambient gas- e.g. the ZrN was produced by ablating the metal under 50 Torr of ammonia. It should be noted that these measurements were made at low pressure; atmospheric pressure measurements may be more challenging. They have also used the inherently quantitative nature of absorption spectroscopy to follow the partitioning of ablated mass among neutral atomic, ionic and molecular "reservoirs" following the ablation of a U3Si2 target under reduced pressures (~10 Torr) of an oxygen-doped Ar atmosphere. Unfortunately, only relative molecular concentrations were measured in this work (see Fig. 11). Absolute measurements of the molecules would require absorption measurements of the entire progression as well as a prior knowledge of the molecular oscillator strengths.

# 4.2.3. Plasma morphology and homogeneity

LA-AS is remarkable for its ability to measure *how much* of a given species is present in a plasma without calibration of an instrument response. Equally important to plume chemistry is understanding *where* the material is in the plasma. The well-defined observation geometry created by coherent probes facilitates this measurement. Where most papers present single-position measurements of the plasma, Martin et al. pulsed laser probes to build two-dimensional maps (they questionably

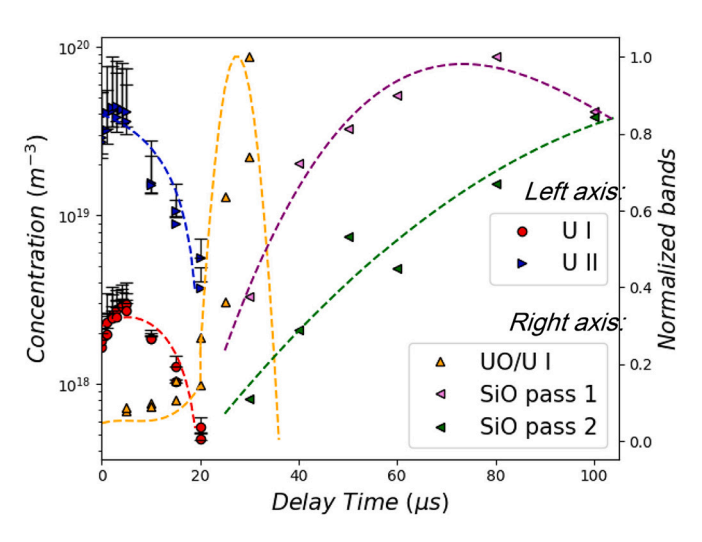


Fig. 11. Temporal evolution of absolute atomic and relative molecular populations following ablation of  $\rm U_3Si_2$  sample at reduced pressure. In the absence of detector gating, early data are optimistic in their implied time resolution given the pulse duration of the flashlamp probe source and absence of detector gating. Reproduced from Reference 36.

refer to them as 3-dimensional) of Mg number densities under PLD ablation conditions [26]. In contrast to the Abel inversions used by Duffey et al. [23] for similarly acquired data, Martin et al. used resonance broadening of the fluorescence signal to calculate number densities [26]. The associated fluorescence data showed a maximum neutral concentration close to the sample surface. Merten has also observed this near-surface maximum in the 2-dimensional CS-AAS measurements that he used to mass the plasma created by ablation of Ti well away from PLD conditions (under 1 atm of helium) [46]. Martin suggests that this maximum at the target surface may be the result of delayed evaporation of material from hot droplets ejected from the sample given that the bulk surface should cool on a picosecond timescale. Merten's neutral Ti measurements (see Fig. 12) show a hollow morphology, with the majority of the ground state number density appearing at the interface between the plasma and the surrounding helium atmosphere or sample surface, a detail not captured by parallel thermal emission measurements.

More recently, Lahaye et al. found that Boltzmann excitation temperatures (measured via emission spectroscopy) and Ca<sup>+</sup> Doppler temperatures (measured in absorption) were relatively congruent while Doppler temperatures from aluminum neutral absorption peaks were significantly lower [73]. Though the neutral and ion absorption measurements shared a line of sight, they likely represent different radial portions of an inhomogeneous plasma and showcase the contrasting view of the LIP provided by absorption spectroscopy. Hopefully, future combination measurements of absorption and emission measurements will allow a more nuanced and complete understanding of plasma formation and evolution.

# 5. Outlook

Among the isotope ratio measurements, more work is needed to fully clarify the source(s) of the time-dependence of the measured ratio-linearity, selectivity or possibly, though less likely in this author's estimation, spatial segregation of the isotopes in a time-of-flight effect. Ideally, further improvements in linear dynamic range will facilitate these experiments and usher in new potential applications. Specifically, this author is keen to see attempts at isotope ratio measurements made from molecular absorption spectra in the LIP. The richness of transitions in the progression might provide a solution to the linear dynamic range problem if individual lines are well resolved. In general, progress in

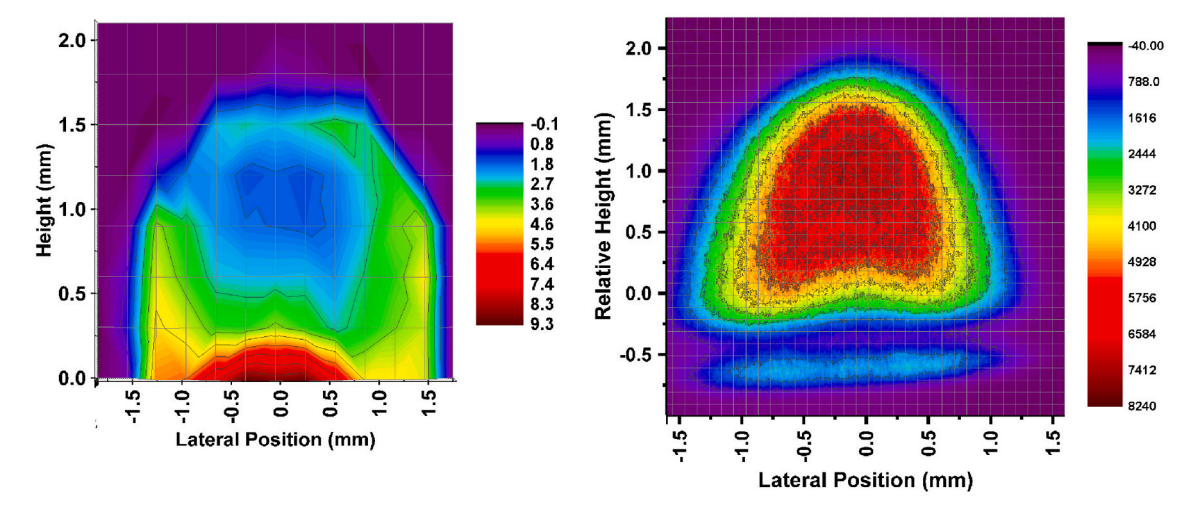


Fig. 12. Contrasting morphologies of ground state neutral Ti absorption (L) and spectrally integrated emission (R) following ablation of pure metal sample under 1 atm of He. Reproduced from Reference 46.

isotope ratio measurements is slowed by the difficulty of standardsaccess to isotopically enriched actinides in relevant quantities/concentrations is understandably restricted and few other elements have experimentally appropriate isotope shifts. An effort to generate a series of lithium isotope ablation standards might benefit studies of this application outside of national laboratories.

This author is particularly sanguine about the use of spatially resolved LA-AS to understand the origin and fate of material in the LIP and analogs. In particular, absolute measurements could allow improved and dynamic understanding of the origin and fate of material through comparison to the crater and other static measures of the ablation process. Spatially resolved absolute measurements of molecular bands and atomic lines should be used to inform plasma modeling and probe the origin of matrix effects in LIBS and LA-ICP measurements. Though it is potentially due to the experimental difficulty (in this author's experience), there are relatively few LA-AS measurements at atmospheric pressure. Hopefully, these measurements will become more common as the LA-AS techniques continue to develop.

Both isotope ratio and plasma diagnostics stand to benefit from a better understanding of noise sources and figures of merit among the different paradigms for LA-AS measurements. Of course, such measurements, or simply measurements in general, have proven difficult to standardize and compare between LIP researchers. Happily, the LIBS community has recently begun to address some of this issue with roundrobin (interlaboratory comparison) campaigns. Analogous efforts might eventually benefit the LA-AS subcommunity. At a minimum, the importance of these figures of merit in LA-AS calls for continued attention from authors and reviewers to clear communication of measurement details in publications.

# **Declaration of Competing Interest**

I declare that I do not have competing interests that could affect this manuscript.

# Acknowledgements

This work is based on work supported by the National Science Foundation under grant number 1905301 and as part of sponsored research funded by the Defense Threat Reduction Agency (DTRA) under grant HDTRA1-16-1-0003. The author wishes to thank George Chan for his generous assistance with the manuscript.

#### References

- J.A. Aguilera, C. Aragón, Characterization of a laser-induced plasma by spatially resolved spectroscopy of neutral atom and ion emissions: Comparison of local and spatially integrated measurements, Spectrochim. Acta Part B: Atom. Spectrosc. 59 (2004) 1861–1876.
- [2] I.B. Gornushkin, S. Shabanov, S. Merk, E. Tognoni, U. Panne, Effects of non-uniformity of laser induced plasma on plasma temperature and concentrations determined by the Boltzmann plot method: implications from plasma modeling, J. Anal. At. Spectrom. 25 (2010) 1643–1653.
- [3] J.T. Costello, J.-P. Mosnier, E.T. Kennedy, P. Carroll, G. O'Sullivan, X-UV absorption spectroscopy with laser-produced plasmas: a review, Phys. Scr. 1991 (1991) 77.
- [4] D.W. Hahn, N. Omenetto, Laser-induced breakdown spectroscopy (LIBS), part I: review of basic diagnostics and plasma-particle interactions: still-challenging issues within the analytical plasma community, Appl. Spectrosc. 64 (2010) 335A-366A
- [5] I.B. Gornushkin, U. Panne, Radiative models of laser-induced plasma and pumpprobe diagnostics relevant to laser-induced breakdown spectroscopy, Spectrochim. Acta Part B: Atom. Spectrosc. 65 (2010) 345–359.
- [6] S.S. Harilal, B.E. Brumfield, N.L. LaHaye, K.C. Hartig, M.C. Phillips, Optical spectroscopy of laser-produced plasmas for standoff isotopic analysis, Appl. Phys. Rev. 5 (2018), 021301.
- [7] B. Welz, M. Sperling, Atomic absorption spectrometry, John Wiley & Sons, 1999.
- [8] I.B. Gornushkin, L.A. King, B.W. Smith, N. Omenetto, J.D. Winefordner, Line broadening mechanisms in the low pressure laser-induced plasma, Spectrochim. Acta Part B: Atom. Spectrosc. 54 (1999) 1207–1217.
- [9] B. Welz, H. Becker-Ross, S. Florek, U. Heitmann, High-Resolution Continuum Source AAS: The Better Way to Do Atomic Absorption Spectrometry, Wiley-VCH, Weinheim, 2005.
- [10] L. King, I. Gornushkin, D. Pappas, B. Smith, J. Winefordner, Rubidium isotope measurements in solid samples by laser ablation-laser atomic absorption spectroscopy, Spectrochim. Acta Part B: Atom. Spectrosc. 54 (1999) 1771–1781.
- [11] J.D. Ingle, S.R. Crouch, Spectrochemical Analysis, Prentice Hall, New Jersey, 1988.
- [12] A. El-Astal, T. Morrow, Wavelength dependent refractive effects and Stark broadening in laser-induced YBa2Cu3O plasma plumes, J. Appl. Phys. 80 (1996) 1156–1160.
- [13] F.J. Gordillo-Vázquez, Concentration of Li atoms in plasmas produced from laser ablation of LiNbO3, J. Appl. Phys. 90 (2001) 599–606.
- [14] H.Y. Moon, K.K. Herrera, N. Omenetto, B.W. Smith, J.D. Winefordner, On the usefulness of a duplicating mirror to evaluate self-absorption effects in laser induced breakdown spectroscopy, Spectrochim. Acta Part B: Atom. Spectrosc. 64 (2009) 702–713.
- [15] B. Smith, A. Quentmeier, M. Bolshov, K. Niemax, Measurement of uranium isotope ratios in solid samples using laser ablation and diode laser-excited atomic fluorescence spectrometry, Spectrochim. Acta Part B: Atom. Spectrosc. 54 (1999) 943–958.
- [16] N.R. Taylor, M.C. Phillips, Differential laser absorption spectroscopy of uranium in an atmospheric pressure laser-induced plasma, Opt. Lett. 39 (2014) 594–597.
- [17] P.J. Skrodzki, N.P. Shah, N. Taylor, K.C. Hartig, N.L. LaHaye, B.E. Brumfield, I. Jovanovic, M.C. Phillips, S.S. Harilal, Significance of ambient conditions in uranium absorption and emission features of laser ablation plasmas, Spectrochim. Acta Part B: Atom. Spectrosc. 125 (2016) 112–119.
- [18] B.A. Bushaw, N.C. Anheier, Isotope ratio analysis on micron-sized particles in complex matrices by Laser Ablation-Absorption Ratio Spectrometry, Spectrochim. Acta Part B: Atom. Spectrosc. 64 (2009) 1259–1265.

- [19] H. Liu, A. Quentmeier, K. Niemax, Diode laser absorption measurement of uranium isotope ratios in solid samples using laser ablation, Spectrochim. Acta Part B: Atom. Spectrosc. 57 (2002) 1611–1623.
- [20] B. Lauly, Diode laser diagnostics of laser-induced plasmas and atomic vapor cells, University of Florida, 2008.
- [21] P.L. Ventzek, R.M. Gilgenbach, C.H. Ching, R.A. Lindley, Schlieren and dye laser resonance absorption photographic investigations of KrF excimer laser-ablated atoms and molecules from polyimide, polyethyleneterephthalate, and aluminum, J. Appl. Physiol. 72 (1992) 1696–1706.
- [22] R.M. Gilgenbach, P.L.G. Ventzek, Dynamics of excimer laser-ablated aluminum neutral atom plume measured by dye laser resonance absorption photography, Appl. Phys. Lett. 58 (1991) 1597–1599.
- [23] T. Duffey, T. McNeela, T. Yamamoto, J. Mazumder, A. Schawlow, Absorption spectroscopic measurements of plume density and temperature in production of nanocrystalline NbAl3 by laser ablation deposition, Phys. Rev. B 51 (1995) 14652.
- [24] H. Sakeek, T. Morrow, W. Graham, D. Walmsley, Optical absorption spectroscopy study of the role of plasma chemistry in YBa2Cu3O7 pulsed laser deposition, Appl. Phys. Lett. 59 (1991) 3631–3633.
- [25] R. Al-Wazzan, C. Lewis, T. Morrow, A technique for mapping three-dimensional number densities of species in laser produced plumes, Rev. Sci. Instrum. 67 (1996) 85–88
- [26] G. Martin, L. Doyle, A. Al-Khateeb, I. Weaver, D. Riley, M. Lamb, T. Morrow, C. Lewis, Three-dimensional number density mapping in the plume of a low-temperature laser-ablated magnesium plasma, Appl. Surf. Sci. 127 (1998) 710–715.
- [27] T. Williamson, G. Martin, A. El-Astal, A. Al-Khateeb, I. Weaver, D. Riley, M. Lamb, T. Morrow, C. Lewis, An investigation of neutral and ion number densities within laser-produced titanium plasmas in vacuum and ambient environments, Appl. Phys. A Mater. Sci. Process. 69 (1999) S859–S863.
- [28] G. Martin, I. Weaver, T. Williamson, A. El-Astal, D. Riley, M. Lamb, T. Morrow, C. Lewis, Study of ground-state titanium ion velocity distributions in laserproduced plasma plumes, Appl. Phys. Lett. 74 (1999) 3465–3467.
- [29] N. Krstulović, N. Čutić, S. Milošević, Spatial and temporal probing of a laser-induced plasma plume by cavity ringdown spectroscopy, Spectrochim. Acta Part B: Atom. Spectrosc. 63 (2008) 1233–1239.
- [30] M. Ribière, B.G. Chéron, Analysis of relaxing laser-induced plasmas by absorption spectroscopy: Toward a new quantitative diagnostic technique, Spectrochim. Acta Part B: Atom. Spectrosc. 65 (2010) 524–532.
- [31] L. Nagli, M. Gaft, I. Gornushkin, Fraunhofer-type absorption lines in double-pulse laser-induced plasma, Appl. Opt. 51 (2012) B201–B212.
- [32] L. Nagli, M. Gaft, Fraunhofer-type absorption line splitting and polarization in confocal double-pulse laser induced plasma, Spectrochim. Acta Part B: Atom. Spectrosc. 88 (2013) 127–135.
- [33] M. Ribière, L. Mées, D. Allano, B. Chéron, Evolutions in time and space of laser ablated species by dual-laser photoabsorption spectroscopy, J. Appl. Physiol. 104 (2008), 043302.
- [34] M. Cui, Y. Deguchi, Z. Wang, S. Tanaka, B. Xue, C. Yao, D. Zhang, Fraunhofer-type signal for underwater measurement of copper sample using collinear long-short double-pulse laser-induced breakdown spectroscopy, Spectrochim. Acta Part B: Atom. Spectrosc. 168 (2020) 105873.
- [35] M. Cui, Y. Deguchi, G. Li, Z. Wang, H. Guo, Z. Qin, C. Yao, D. Zhang, Determination of manganese in submerged steel using Fraunhofer-type line generated by longshort double-pulse laser-induced breakdown spectroscopy, Spectrochim. Acta Part B: Atom. Spectrosc. 180 (2021) 106210.
- [36] E.N. Weerakkody, D.G. Weisz, J. Crowhurst, B. Koroglu, T. Rose, H. Radousky, R. L. Stillwell, J.R. Jeffries, N.G. Glumac, Time-resolved formation of uranium and silicon oxides subsequent to the laser ablation of U3Si2, Spectrochim. Acta Part B: Atom. Spectrosc. 170 (2020) 105925.
- [37] T. Morrow, H. Sakeek, A. El Astal, W. Graham, D. Walmsley, Absorption and emission spectra of the YBCO laser plume, J. Supercond. 7 (1994) 823–828.
- [38] D.B. Geohegan, A.A. Puretzky, Dynamics of laser ablation plume penetration through low pressure background gases, Appl. Phys. Lett. 67 (1995) 197–199.
- [39] A. El-Astal, T. Morrow, W. Graham, D. Walmsley, The role of gas-phase oxidation and combination during laser deposition of YBa2Cu3O7-x in ambient oxygen, Supercond. Sci. Technol. 8 (1995) 529.
- [40] E. Weerakkody, N. Glumac, Quantitative absorption spectroscopy of laser-produced plasmas, J. Phys. D. Appl. Phys. (2021) 54.
- [41] A.A. Puretzky, D.B. Geohegan, Laser ablation plume thermalization dynamics in background gases: combined imaging, optical absorption and emission spectroscopy, and ion probe measurements, Appl. Surf. Sci. 127 (1998) 248–254.
- [42] A.A. Puretzky, D.B. Geohegan, Gas-phase diagnostics and LIF-imaging of 3hydroxypicolinic acid MALDI-matrix plumes, Chem. Phys. Lett. 286 (1998) 425–432.
- [43] N. Glumac, Absorption Spectroscopy Measurements in Optically Dense Explosive Fireballs Using a Modeless Broadband Dye Laser, Appl. Spectrosc. 63 (2009) 1075–1080.
- [44] M. Soo, N. Glumac, Ultraviolet Absorption Spectroscopy in Optically Dense Fireballs Using Broadband Second-Harmonic Generation of a Pulsed Modeless Dye Laser, Appl. Spectrosc. 68 (2014) 517–524.
- [45] J. Merten, B. Johnson, Laser continuum source atomic absorption spectroscopy: Measuring the ground state with nanosecond resolution in laser-induced plasmas, Spectrochim. Acta Part B: Atom. Spectrosc. 139 (2018) 38–43.

- [46] J. Merten, B. Johnson, Massing a laser-induced plasma with atomic absorption spectroscopy, Spectrochim. Acta Part B: Atom. Spectrosc. 149 (2018) 124–131.
- [47] J. Bergevin, T.-H. Wu, J. Yeak, B.E. Brumfield, S.S. Harilal, M.C. Phillips, R. J. Jones, Dual-comb spectroscopy of laser-induced plasmas, Nat. Commun. 9 (2018) 1–6.
- [48] Y. Zhang, R.R. Weeks, C. Lecaplain, S. Harilal, J. Yeak, M. Phillips, R.J. Jones, Burst-mode dual-comb spectroscopy, Opt. Lett. 46 (2021) 860–863.
- [49] Y. Zhang, C. Lecaplain, R.R. Weeks, J. Yeak, S.S. Harilal, M.C. Phillips, R.J. Jones, Time-resolved dual-comb measurement of number density and temperature in a laser-induced plasma, Opt. Lett. 44 (2019) 3458–3461.
- [50] Y. Zhang, R.R. Weeks, C. Lecaplain, J. Yeak, S.S. Harilal, M.C. Phillips, R.J. Jones, Pulse burst mode dual-comb spectroscopy for time-resolved measurements of laserinduced plasmas, Science and Innovations, CLEO, 2020.
- [51] R.R.D. Weeks, M.C. Phillips, Y. Zhang, S.S. Harilal, R.J. Jones, Measurement of neutral gadolinium oscillator strengths using dual-comb absorption spectroscopy in laser-produced plasmas, Spectrochim. Acta Part B: Atom. Spectrosc. 181 (2021) 106199.
- [52] I. Coddington, N. Newbury, W. Swann, Dual-comb spectroscopy, Optica 3 (2016) 414–426.
- [53] N.R. Newbury, I. Coddington, W. Swann, Sensitivity of coherent dual-comb spectroscopy, Opt. Express 18 (2010) 7929–7945.
- [54] Y. Zhang, R.R.D. Weeks, C. Lecaplain, S.S. Harilal, J. Yeak, M.C. Phillips, R. J. Jones, Burst-mode dual-comb spectroscopy, Opt. Lett. 46 (2021) 860–863.
- [55] M. Miyabe, M. Oba, H. Iimura, K. Akaoka, Y. Maruyama, H. Ohba, M. Tampo, I. Wakaida, Doppler-shifted optical absorption characterization of plume-lateral expansion in laser ablation of a cerium target, J. Appl. Phys. 112 (2012) 123303.
- [56] M. Miyabe, M. Oba, H. Iimura, K. Akaoka, Y. Maruyama, I. Wakaida, Spectroscopy of laser-produced cerium plasma for remote isotope analysis of nuclear fuel, Appl. Phys. A Mater. Sci. Process. 101 (2010) 65–70.
- [57] M. Miyabe, M. Oba, K. Akaoka, M. Kato, S. Hasegawa, I. Wakaida, Development of laser ablation absorption spectroscopy for nuclear fuel materials: plume expansion behavior for refractory metals observed by laser-induced fluorescence imaging spectroscopy, Appl. Phys. A Mater. Sci. Process. 126 (2020) 213.
- [58] G. Hull, E.D. McNaghten, P. Coffey, P. Martin, Isotopic analysis and plasma diagnostics for lithium detection using combined laser ablation-tuneable diode laser absorption spectroscopy and laser-induced breakdown spectroscopy, Spectrochim. Acta Part B: Atom. Spectrosc. 177 (2021) 106051.
- [59] M. Miyabe, M. Oba, K. Jung, H. Iimura, K. Akaoka, M. Kato, H. Otobe, A. Khumaeni, I. Wakaida, Laser ablation absorption spectroscopy for isotopic analysis of plutonium: Spectroscopic properties and analytical performance, Spectrochim. Acta - Part B Atom. Spectrosc. 134 (2017) 42–51.
- [60] S. Harilal, E. Kautz, M. Phillips, Time-resolved absorption spectroscopic characterization of ultrafast laser-produced plasmas under varying background pressures, Phys. Rev. E 103 (2021), 013213.
- [61] S.S. Harilal, E.J. Kautz, R.J. Jones, M.C. Phillips, Spectro-temporal comparisons of optical emission, absorption, and laser-induced fluorescence for characterizing ns and fs laser-produced plasmas, Plasma Sources Sci. Technol. 30 (2021), 045007.
- [62] B.A. Bushaw, M.L. Alexander, Investigation of laser ablation plume dynamics by high-resolution time-resolved atomic absorption spectroscopy, Appl. Surf. Sci. 127 (1998) 935–940.
- [63] N. Krstulović, N. Čutić, S. Milošević, Cavity ringdown spectroscopy of collinear dual-pulse laser plasmas in vacuum, Spectrochim. Acta Part B: Atom. Spectrosc. 64 (2009) 271–277.
- [64] M. Bišćan, S. Milošević, Expansion and backscattering of laser produced Fe plasma plume, Spectrochim. Acta Part B: Atom. Spectrosc. 68 (2012) 34–39.
- [65] M. Miyabe, M. Oba, H. Iimura, K. Akaoka, A. Khumaeni, M. Kato, I. Wakaida, Ablation plume structure and dynamics in ambient gas observed by laser-induced fluorescence imaging spectroscopy, Spectrochim. Acta Part B: Atom. Spectrosc. 110 (2015) 101–117.
- [66] S.S. Harilal, C.M. Murzyn, M.C. Phillips, J.B. Martin, Hyperfine structures and isotopic shifts of uranium transitions using tunable laser spectroscopy of laser ablation plumes, Spectrochim. Acta Part B: Atom. Spectrosc. 169 (2020) 105828.
- [67] N. Cheung, Q. Ying, J. Zheng, H.S. Kwok, Time-resolved resonant absorption study of 532-nm laser-generated plumes over YBa2Cu3O7 targets, J. Appl. Phys. 69 (1991) 6349–6354.
- [68] D.B. Geohegan, A.A. Puretzky, Laser ablation plume thermalization dynamics in background gases: combined imaging, optical absorption and emission spectroscopy, and ion probe measurements, Appl. Surf. Sci. 96 (1996) 131–138.
- [69] R. Wood, K.-R. Chen, J. Leboeuf, A. Puretzky, D. Geohegan, Dynamics of plume propagation and splitting during pulsed-laser ablation, Phys. Rev. Lett. 79 (1997) 1571.
- [70] M. Bišćan, S. Milošević, Production of metastable 23S1 helium in a laser produced plasma at low pressures, Spectrochim. Acta Part B: Atom. Spectrosc. 81 (2013) 20–25.
- [71] I. Labazan, S. Milošević, Laser vaporized Li2, Na2, K2, and LiNa molecules observed by cavity ring-down spectroscopy, Phys. Rev. A 68 (2003), 032901.
- [72] M.G. Tarallo, G.Z. Iwata, T. Zelevinsky, BaH molecular spectroscopy with relevance to laser cooling, Phys. Rev. A 93 (2016), 032509.
- [73] N.L. LaHaye, S.S. Harilal, M.C. Phillips, Early- and late-time dynamics of laser-produced plasmas by combining emission and absorption spectroscopy, Spectrochim. Acta Part B: Atom. Spectrosc. 179 (2021) 106096.